Available online at www.sciencedirect.com
SCIENCE DIRECT
Journal of Sound and Vibration 296 (2006) 746–756
JOURNAL OF SOUND AND VIBRATION
www.elsevier.com/locate/jsvi

Analysis of nonlinear vibration for embedded carbon nanotubes

Y.M. Fu, J.W. Hong, X.Q. Wang*

Department of Engineering Mechanics Hunan University, Changsha, Hunan, China

Received 13 July 2004; received in revised form 21 December 2004; accepted 3 February 2006
Available online 23 May 2006

Abstract

Based on the continuum mechanics and a multiple-elastic beam model, the nonlinear free vibration of embedded multi-wall carbon nanotubes considering intertube radial displacement and the related internal degrees of freedom is investigated. By using the incremental harmonic balanced method, the iterative relationship of nonlinear amplitude and frequency for the single-wall nanotube and double-wall nanotube are expressed. In the numerical calculation, the amplitude frequency response curves of the nonlinear free vibration for the single-wall and double-wall nanotubes are obtained. The effects of the surrounding elastic medium, van der Waals forces and aspect ratio of the multi-wall nanotubes on the amplitude frequency response characteristics are discussed.

1. Introduction

The discovery of carbon nanotubes (CNT) by Iijima [1], especially the discovery of the single-wall nanotube (SWNT) and the successful composition of the CNT in the macrography scale, has received considerable attention in recent years. At the present CNT has been the chief research subject in the area of the fullerene, and it has been one of the most promising researches in the field of mechanics, physics, chemistry and materials science, etc. Because of their novel electronic, mechanical, and other physical and chemical properties, CNT holds substantial promise as building blocks for nanoelectronics, nanodevices, and nanocomposites. For example, the stiffness of CNT is 100 times as that of the steel, but the weight is one-sixth times as that of the steel [2]. It is foreseen to be the most promising one-dimensional nanophase materials in the 21st century. Therefore, it is necessary and significant to study its mechanical property.

Various buckling and bending problems of CNT have been investigated by using experimental method and molecular-dynamics simulations [3–9]. In many proposed applications and designs, CNTs are often embedded in another elastic medium, therefore, considerable attention is focused on mechanical behaviors of CNTs embedded in a polymer or metal matrix [7]. But the single-beam model used in these literatures neglects the intertube radial displacement, the related internal degrees of freedom and van der Waals forces which inevitably cause internal non-coaxial deformation and distort the otherwise concentric geometry of multi-wall nanotube (MWNT). Especially, because each of the nested tubes of a MWNT could have different electronic

*Corresponding author.
E-mail address: xqwang_1022@163.com (X.Q. Wang).

0022-460X/$ - see front matter © 2006 Elsevier Ltd. All rights reserved.
doi:10.1016/j.jsv.2006.02.024

properties, non-coaxial distortion could significantly affect some important physical properties of MWNT. Therefore, it is necessary to understand intertube vibration of embedded MWNT. Based on the non-coaxial vibrational model of MWNT, Ru [10] studied the bulking of nanotubes. Considering the intertube radial displacement and the internal van der Waals forces, Yoon and Ru [11] analyzed the frequencies and models of the linear free vibration for the embedded MWNT. To our knowledge, the nonlinear free vibration of embedded nanotubes has not been studied in the literatures.

The deformations of nanostructure, such as CNTs, as the same as those of the macroscopic structures are nonlinear in nature under the action of the external conditions. Only when taking into account the nonlinearities in geometry and physics, the more static and dynamic properties of nanostructure can be obtained and then the nanostructures can receive more wide applications. In this paper, the nonlinear free vibration analysis of CNTs considering the geometric nonlinearity is investigated. The main reasons of considering the nonlinearity and useful examples are as follows:

First, the nonlinear amplitude frequency response, the bifurcate and chaos of the nanostructure can be investigated in the nonlinear model rather than in the linear model.

Second, the more precise mechanical properties can be obtained. For example, when measuring the Young's modulus of CNT by using the vibration method, the experiment value can be consistent with the theoretical value only under considering the nonlinear deformation of CNT. Another case is that when weighing the nanoscale materials by adopting the nano-steelyard, the more precise mass is obtained when taking into account the geometric nonlinearity of CNT.

Moreover, the nonlinear mechanical behavior of CNT has received considerable attentions in recent years. For example, Pantano and Boyce [12] investigated the effect of the characteristic wavelike or wrinkles on the bending mode of CNT under considering the geometric nonlinearity and explained the phenomenon that the curve modes of CNT decrease with the increase of the diameter of CNT.

In this paper, based on the continuum mechanics and a multiple-elastic beam model, the nonlinear free vibration analysis of embedded CNT considering intertube radial displacement and the related internal degrees of freedom is investigated.

2. Basic equations

There are two simplified methods in modeling CNTs based on the continuum mechanics at present. One is to simplify every layer of the tube to contact the adjacent tube and the distance of the adjacent layer may be neglected. In this model, the thickness t_0 of the every layer of the tube is 0.34 nm and the Young's modulus is 1.1 TPa. The other model is that the interlayer spacing between every adjacent tube is 0.34 nm and the thickness of the tube t_0 is 0.066 nm, the Young's modulus is 5.5 TPa. The later is usually applied to the CNTs with small aspect ratio and in this model, the tubes is treated as the shell [13]. In present research, the aspect ratios of nanotubes are all beyond 10, so the former model is employed.

Consider a CNT of length l, Young's modulus E, density ρ, cross-sectional area A, and cross-sectional inertia moment I, embedded in elastic medium as shown in Fig. 1. Assume that the displacement of nanotube along x axial is $u(x,t)$, and the displacement along z axial is $w(x,t)$ in terms of the spatial coordinate x and the time variable t. The free vibration equation of embedded nanotube considering the geometric nonlinearity of

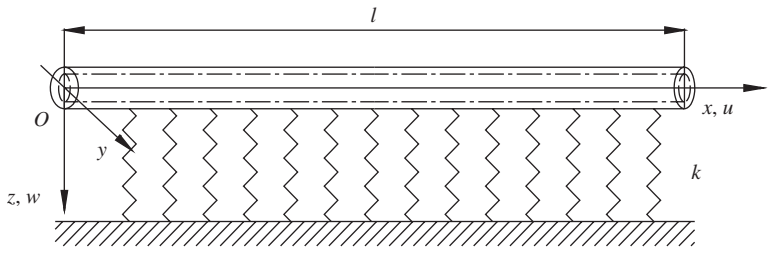

Fig. 1. Model of an embedded carbon nanotube.

the structure is

$$EI\frac{\mathrm{d}^4w}{\mathrm{d}x^4}+\rho A\frac{\mathrm{d}^2w}{\mathrm{d}t^2}=\left[\frac{EA}{2l}\int_0^l\left(\frac{\partial w}{\partial x}\right)\mathrm{d}x\right]\frac{\partial^2w}{\partial x^2}+p, \tag{1}$$

where $p(x,t)$ is the interaction pressure per unit axial length between the outermost tube and the surrounding medium, which can be described by the Winkler-like model [14,15], and

$$p=-kw, \tag{2}$$

where the negative sign indicates that the pressure p is opposite to the deflection of the outmost tube, and k is a constant determined by the material constants of the surrounding elastic medium. Substituting Eq. (2) into Eq. (1), that gives

$$EI\frac{\mathrm{d}^4w}{\mathrm{d}x^4}+\rho A\frac{\mathrm{d}^2w}{\mathrm{d}t^2}+kw=\left[\frac{EA}{2l}\int_0^l\left(\frac{\partial w}{\partial x}\right)\mathrm{d}x\right]\frac{\partial^2w}{\partial x^2}. \tag{3}$$

Assume that the nanotube is simply supported at the two ends. So, the unknown function $w(x,t)$ may be given as

$$w(x,t)=W(t)\sin\frac{\pi x}{l}. \tag{4}$$

It satisfies the boundary condition: $x=0,\ l:w=0,\ M=0$, in which M is the stress couple. By substituting Eq. (4) into Eq. (3), the nonlinear differential equation for the time function $W(t)$ can be obtained as follows:

$$\frac{\mathrm{d}^2W}{\mathrm{d}t^2}+\left(\frac{\pi^4EI}{l^4\rho A}+\frac{k}{\rho A}\right)W+\frac{\pi^4E}{4l^4\rho}W^3=0. \tag{5}$$

For the MWNT with N layers, the pressure at any point between any two adjacent tubes depends on the difference of their deflections at that point. Thus the van der Waals force can be expressed as

$$F_i=c_i(w_i-w_{i-1}), \tag{6}$$

where F_i is the van der Waals force between the ith tube and the $i-1$th tube. c_i is the coefficient of the van der Waals force between the ith tube and the $i-1$th tube. And c_i can be defined by [10]

$$c_i=\frac{200\times(2r_{i-1})\ \mathrm{erg/cm^2}}{0.16d^2}\quad(i=2,3,\ldots,N), \tag{7}$$

in which $d=0.142\,\mathrm{nm}$, r_{i-1} is the radius of ith tube.

Assume that all nested individual tubes of the MWNT vibrate in the same plane. Considering the effects of the van der Waals forces in Eq. (3), the coplanar transverse nonlinear free vibration of an embedded MWNT with N layers is described by the following N coupled nonlinear differential equations:

$$\begin{aligned}
&EI_1\frac{\mathrm{d}^4w_1}{\mathrm{d}x^4}+\rho A_1\frac{\mathrm{d}^2w_1}{\mathrm{d}t^2}=\left[\frac{EA_1}{2l}\int_0^l\left(\frac{\partial w_1}{\partial x}\right)\mathrm{d}x\right]\frac{\partial^2w_1}{\partial x^2}+c_1[w_2-w_1],\\
&EI_2\frac{\mathrm{d}^4w_2}{\mathrm{d}x^4}+\rho A_2\frac{\mathrm{d}^2w_2}{\mathrm{d}t^2}=\left[\frac{EA_2}{2l}\int_0^l\left(\frac{\partial w_2}{\partial x}\right)\mathrm{d}x\right]\frac{\partial^2w_2}{\partial x^2}+c_2[w_3-w_2]-c_1[w_2-w_1],\\
&\vdots\\
&EI_N\frac{\mathrm{d}^4w_N}{\mathrm{d}x^4}+\rho A_N\frac{\mathrm{d}^2w_N}{\mathrm{d}t^2}=\left[\frac{EA_N}{2l}\int_0^l\left(\frac{\partial w_N}{\partial x}\right)\mathrm{d}x\right]\frac{\partial^2w_N}{\partial x^2}-c_{N-1}[w_N-w_{N-1}]-kw_N.
\end{aligned} \tag{8}$$

By using the former simplified method for the MWNT having simply supported condition at the two ends, the nonlinear vibration equations of an embedded MWNT with N layers can be written in term of the time

function $W_i(t)$ as

$$\begin{aligned}
&\frac{d^2W_1}{dt^2}+\left(\frac{\pi^4EI_1}{l^4\rho A_1}+\frac{c_1}{\rho A_1}\right)W_1+\frac{\pi^4E}{4l^4\rho}W_1^3-\frac{c_1}{\rho A_1}W_2=0,\\
&\frac{d^2W_2}{dt^2}+\left(\frac{\pi^4EI_2}{l^4\rho A_2}+\frac{c_1}{\rho A_2}+\frac{c_2}{\rho A_2}\right)W_2+\frac{\pi^4E}{4l^4\rho}W_2^3-\frac{c_1}{\rho A_2}W_1-\frac{c_2}{\rho A_2}W_3=0,\\
&\vdots\\
&\frac{d^2W_N}{dt^2}+\left(\frac{\pi^4EI_N}{l^4\rho A_N}+\frac{c_{N-1}}{\rho A_N}+\frac{k}{\rho A_N}\right)W_N+\frac{\pi^4E}{4l^4\rho}W_N^3-\frac{c_{N-1}}{\rho A_N}W_{N-1}=0.
\end{aligned}\tag{9}$$

3. Solution methodology

3.1. Solutions of SWNT

For a SWNT, the nonlinear vibration governing equation is given by Eq. (9) with $N=1$ as follows:

$$\frac{d^2W}{dt^2}+\left(\frac{\pi^4EI}{l^4\rho A}+\frac{k}{\rho A}\right)W+\frac{\pi^4E}{4l^4\rho}W^3=0.\tag{10}$$

Introducing the dimensionless parameters: $r=\sqrt{I/A}$, $a=W/r$, $\omega_l=\pi^2/l^2\sqrt{EI/\rho A}$, $\omega_k=\sqrt{k/\rho A}$, $\tau=\omega t$, substituting these into Eq. (10), the dimensionless nonlinear vibration governing equation is given as

$$\left(\frac{\omega}{\omega_l}\right)^2\frac{d^2a}{d\tau^2}+\left[1+\left(\frac{\omega_k}{\omega_l}\right)^2\right]a+\alpha a^3=0,\tag{11}$$

where $\alpha=0.25$. Eq. (11) is the famous Duffing equation. Generally, the analytical solution of Eq. (11) is hard to find out. In present analysis, a high precision method, the incremental harmonic balanced method [16] is employed to seek the numerical solution of Eq. (11).

Assume $a_0(\tau)$ and ω_0 to be a known vibration status, that is, they are the known solutions of Eq. (11). Then a neighboring vibration status with the amplitude increment $\Delta a(t)$ and the frequency increment $\Delta\omega$ can be expressed as

$$a(\tau)=a_0(\tau)+\Delta a(\tau),\quad \omega=\omega_0+\Delta\omega.\tag{12}$$

Substituting Eq. (12) in Eq. (11) and neglecting the high-order microcontent, a linearized increment equation can be expressed as

$$\left(\frac{\omega_0}{\omega_l}\right)^2\frac{d^2\Delta a}{d\tau^2}+\left[1+\left(\frac{\omega_k}{\omega_l}\right)^2\right]\Delta a+3\alpha a_0^2\Delta a=R-2\left(\frac{\omega_0}{\omega_l}\right)\left(\frac{\Delta\omega}{\omega_l}\right)\frac{d^2a_0}{d\tau^2},\tag{13}$$

where

$$R=-\left(\frac{\omega_0}{\omega_l}\right)^2\frac{d^2a_0}{d\tau^2}-\left[1+\left(\frac{\omega_k}{\omega_l}\right)^2\right]a_0-\alpha a_0^3\tag{14}$$

and it is the corrective term, that is, it will become zero if $a_0(\tau)$ and ω_0 are the exact solutions of Eq. (11).

In order to seek the periodic solutions of Eq. (11), the functions $a_0(\tau)$ and $\Delta a(\tau)$ can be taken in the form of cosine harmonic wave as

$$\begin{aligned}
a_0&=a_1\cos\tau+a_3\cos 3\tau+\cdots,\\
\Delta a&=\Delta a_1\cos\tau+\Delta a_3\cos 3\tau+\cdots.
\end{aligned}\tag{15}$$

Substituting Eq. (15) in Eq. (13) and equating the coefficient of the same harmonic wave terms, the matrix algebra equation can be got as follows:

$$([K]-\left(\frac{\omega_0}{\omega_l}\right)^2[M]+\left(\frac{\omega_k}{\omega_l}\right)^2[P])\begin{Bmatrix}\Delta a_1\\ \Delta a_3\end{Bmatrix}=\begin{bmatrix}R_1\\ R_3\end{bmatrix}+\left(\frac{\Delta\omega}{\omega_l}\right)\begin{Bmatrix}F_1\\ F_3\end{Bmatrix}, \tag{16}$$

where

$$[K]=\begin{bmatrix}K_{11} & K_{13}\\ K_{31} & K_{33}\end{bmatrix},\quad [M]=\begin{bmatrix}m_{11} & m_{13}\\ m_{31} & m_{33}\end{bmatrix},\quad [P]=\begin{bmatrix}p_{11} & p_{13}\\ p_{31} & p_{33}\end{bmatrix},$$

$$K_{11}=1+\frac{3}{2}\alpha\left(\frac{3}{2}a_1^2+a_1a_3+a_3^2\right),\quad K_{13}=\frac{3}{2}\alpha\left(\frac{1}{2}a_1^2+2a_1a_3\right),\quad K_{31}=K_{13},\quad K_{33}=1+\frac{3}{2}\alpha\left(a_1^2+\frac{3}{2}a_3^2\right),$$

$$m_{11}=1,\quad m_{13}=m_{31}=0,\quad m_{33}=9,\quad p_{11}=1,\quad p_{13}=p_{31}=0,\quad p_{33}=1,$$

$$R_1=-a_1-\frac{3}{4}\alpha(a_1^2+a_1a_3+2a_3^2)a_1+\left(\frac{\omega_0}{\omega_l}\right)^2a_1-\left(\frac{\omega_k}{\omega_l}\right)^2a_1,$$

$$R_2=-a_3-\frac{\alpha}{4}(a_1^3+6a_1^2a_3+3a_3^2)+9\left(\frac{\omega_0}{\omega_l}\right)^2a_3-\left(\frac{\omega_k}{\omega_l}\right)^2a_3,$$

$$F_1=2\left(\frac{\omega_0}{\omega_l}\right)a_1,\quad F_3=18\left(\frac{\omega_0}{\omega_l}\right)a_3. \tag{17}$$

Eq. (16) can be solved for Δa_3 and $\Delta\omega$ for the given values of a_1, a_3 and ω_0 and for a given increment Δa_1 in which the corresponding a_1 is set to zero. Consequencely, the next vibration status $a_1+\Delta a_1$, $a_2+\Delta a_2$ and $\omega+\Delta\omega$ can be calculated. Then taking these solutions as a new vibration status and using the former solving process, the nonlinear amplitude frequency response curves can be obtained.

3.2. Solution of double-wall nanotubes (DWNT)

For a DWNT, the nonlinear vibration governing equations are given by Eq. (9) with $N=2$ as follows:

$$\begin{aligned}&\frac{d^2W_1}{dt^2}+\left(\frac{\pi^4EI_1}{l^4\rho A_1}+\frac{c_1}{\rho A_1}\right)W_1+\frac{\pi^4E}{4l^4\rho}W_1^3-\frac{c_1}{\rho A_1}W_2=0,\\ &\frac{d^2W_2}{dt^2}+\left(\frac{\pi^4EI_2}{l^4\rho A_2}+\frac{c_1}{\rho A_2}+\frac{k}{\rho A_2}\right)W_2+\frac{\pi^4E}{4l^4\rho}W_2^3-\frac{c_1}{\rho A_2}W_1=0.\end{aligned} \tag{18}$$

Introducing the following dimensionless parameters:

$$r=\sqrt{\frac{I_1}{A_1}},\quad a_1=\frac{W_1}{r},\quad a_2=\frac{W_2}{r},\quad \omega_l=\frac{\pi^2}{l^2}\sqrt{\frac{EI_1}{\rho A_1}},\quad \omega_k=\sqrt{\frac{k}{\rho A_1}},\quad \omega_c=\sqrt{\frac{c}{\rho A_1}},$$

$$\tau=\omega t,\quad \beta=\frac{A_1}{A_2},\quad \gamma=\frac{I_1}{I_2},\quad \alpha=\frac{1}{4}$$

and substituting these into Eq. (18), the dimensionless nonlinear vibration governing equations are

$$\begin{aligned}&\left(\frac{\omega}{\omega_l}\right)^2\frac{d^2a_1}{d\tau^2}+\left[1+\left(\frac{\omega_c}{\omega_l}\right)^2\right]a_1+\alpha a_1^3-\left(\frac{\omega_c}{\omega_l}\right)^2a_2=0,\\ &\left(\frac{\omega}{\omega_l}\right)^2\frac{d^2a_2}{d\tau^2}+\beta\left[\frac{1}{\gamma}+\left(\frac{\omega_c}{\omega_l}\right)^2+\left(\frac{\omega_k}{\omega_l}\right)^2\right]a_2+\alpha a_2^3-\beta\left(\frac{\omega_c}{\omega_l}\right)^2a_1=0.\end{aligned} \tag{19}$$

Also, the incremental harmonic balanced method is employed to seek solution of Eq. (19). Assume $a_1(\tau)$, $a_2(\tau)$ and ω_0 to be a known vibration status, then a neighboring vibration status with the amplitude

increment Δa_1, Δa_2 and the frequency increment $\Delta\omega$ can be expressed as

$$\begin{aligned} a_1(\tau) &= a_{10}(\tau) + \Delta a_1(\tau), \\ a_2(\tau) &= a_{20}(\tau) + \Delta a_2(\tau), \\ \omega &= \omega_0 + \Delta\omega. \end{aligned} \tag{20}$$

Substituting Eq. (20) in Eq. (19) and neglecting the high-order microcontent, two linearized increment equations can be expressed as

$$\begin{aligned} &\left(\frac{\omega_0}{\omega_l}\right)^2 \frac{\mathrm{d}^2\Delta a_1}{\mathrm{d}\tau^2} + \left[1 + \left(\frac{\omega_c}{\omega_l}\right)^2\right]\Delta a_1 + 3\alpha a_{10}^2 \Delta a_1 - \left(\frac{\omega_c}{\omega_l}\right)^2 \Delta a_2 = R_1 - 2\left(\frac{\omega_0}{\omega_l}\right)\left(\frac{\Delta\omega}{\omega_l}\right)\frac{\mathrm{d}^2 a_{10}}{\mathrm{d}\tau^2}, \\ &\left(\frac{\omega_0}{\omega_l}\right)^2 \frac{\mathrm{d}^2\Delta a_2}{\mathrm{d}\tau^2} + \beta\left[\frac{1}{\gamma} + \left(\frac{\omega_c}{\omega_l}\right)^2 + \left(\frac{\omega_k}{\omega_l}\right)^2\right]\Delta a_2 + 3\alpha a_{20}^2 \Delta a_2 - \beta\left(\frac{\omega_c}{\omega_l}\right)^2 \Delta a_1 = R_2 - 2\left(\frac{\omega_0}{\omega_l}\right)\left(\frac{\Delta\omega}{\omega_l}\right)\frac{\mathrm{d}^2 a_{20}}{\mathrm{d}\tau^2}, \end{aligned} \tag{21}$$

where

$$\begin{aligned} R_1 &= -\left(\frac{\omega_0}{\omega_l}\right)^2 \frac{\mathrm{d}^2 a_{10}}{\mathrm{d}\tau^2} - \left[1 + \left(\frac{\omega_c}{\omega_l}\right)^2\right] a_{10} - \alpha a_{10}^3 + \left(\frac{\omega_c}{\omega_l}\right)^2 a_{20}, \\ R_2 &= -\left(\frac{\omega_0}{\omega_l}\right)^2 \frac{\mathrm{d}^2 a_{20}}{\mathrm{d}\tau^2} - \beta\left[\frac{1}{\gamma} + \left(\frac{\omega_c}{\omega_l}\right)^2 + \left(\frac{\omega_k}{\omega_l}\right)^2\right] a_{20} - \alpha a_{20}^3 + \beta\left(\frac{\omega_c}{\omega_l}\right)^2 a_{10}. \end{aligned} \tag{22}$$

As the front method, the functions a_{10}, Δa_{10}, a_{20}, Δa_{20} can be taken in the form of cosine harmonic wave as

$$\begin{aligned} a_{10} &= a_1 \cos\tau + a_3 \cos 3\tau + \cdots, \quad \Delta a_{10} = \Delta a_1 \cos\tau + \Delta a_3 \cos 3\tau + \cdots, \\ a_{20} &= a_2 \cos\tau + a_4 \cos 3\tau + \cdots, \quad \Delta a_{20} = \Delta a_2 \cos\tau + \Delta a_4 \cos 3\tau + \cdots, \end{aligned} \tag{23}$$

Substituting Eq. (23) into Eq. (21) and equating the coefficient of the same harmonic wave terms, the following matrix algebra equations are obtained:

$$([K] + [W])\begin{Bmatrix} \Delta a_1 \\ \Delta a_2 \\ \Delta a_3 \\ \Delta a_4 \end{Bmatrix} = \begin{bmatrix} R_1 \\ R_2 \\ R_3 \\ R_4 \end{bmatrix} + 2\begin{bmatrix} Q_1 \\ Q_2 \\ Q_3 \\ Q_4 \end{bmatrix}, \tag{24}$$

where

$$[K] = \begin{bmatrix} K_{11} & K_{12} & K_{13} & K_{14} \\ K_{21} & K_{22} & K_{23} & K_{24} \\ K_{31} & K_{32} & K_{33} & K_{34} \\ K_{41} & K_{42} & K_{43} & K_{44} \end{bmatrix},$$

$$K_{11} = 1 + \frac{9}{4}\alpha a_1^2 + \frac{3}{2}\alpha a_1 a_3 + \frac{3}{2}\alpha a_3^2, \quad K_{12} = K_{14} = 0, \quad K_{13} = \frac{3}{4}\alpha a_1^2 + 3\alpha a_1 a_3,$$

$$K_{21} = \frac{3}{4}\alpha a_1^2 + 3\alpha a_1 a_3, \quad K_{22} = K_{24} = 0, \quad K_{23} = 1 + \frac{3}{2}\alpha a_1^2 + \frac{9}{4}\alpha a_3^2,$$

$$K_{31} = K_{33} = 0, \quad K_{32} = \frac{\beta}{\gamma} + \frac{9}{4}\alpha a_2^2 + \frac{3}{2}\alpha a_2 a_4 + \frac{3}{2}\alpha a_4^2, \quad K_{34} = \frac{3}{4}\alpha a_2^2 + 3\alpha a_2 a_4,$$

$$K_{41} = K_{43} = 0, \quad K_{42} = \frac{3}{4}\alpha a_2^2 + 3\alpha a_2 a_4, \quad K_{44} = \frac{\beta}{\gamma} + \frac{3}{2}\alpha a_2^2 + \frac{9}{4}\alpha a_4^2,$$

$$[W]=\begin{bmatrix} -(\frac{\omega_0}{\omega_l})^2+(\frac{\omega_c}{\omega_l})^2 & -(\frac{\omega_c}{\omega_l})^2 & 0 & 0 \\ 0 & 0 & -9(\frac{\omega_0}{\omega_l})^2+(\frac{\omega_c}{\omega_l})^2 & -(\frac{\omega_c}{\omega_l})^2 \\ -\beta(\frac{\omega_c}{\omega_l})^2 & -(\frac{\omega_0}{\omega_l})^2+\beta(\frac{\omega_c}{\omega_l})^2+\beta(\frac{\omega_k}{\omega_l})^2 & 0 & 0 \\ 0 & 0 & -\beta(\frac{\omega_c}{\omega_l})^2 & -9(\frac{\omega_0}{\omega_l})^2+\beta(\frac{\omega_c}{\omega_l})^2+\beta(\frac{\omega_k}{\omega_l})^2 \end{bmatrix},$$

$$R_1=-\left[\frac{3}{4}\alpha a_1^3+\frac{3}{4}\alpha a_1^2a_3+a_1+\frac{3}{2}\alpha a_1a_3^2-a_2\left(\frac{\omega_c}{\omega_l}\right)^2-a_1\left(\frac{\omega_0}{\omega_l}\right)^2+a_1\left(\frac{\omega_c}{\omega_l}\right)^2\right],$$

$$R_2=-\left[\frac{1}{4}\alpha a_1^3+\frac{3}{2}\alpha a_1^2a_3+a_3+\frac{3}{4}\alpha a_3^2-a_4\left(\frac{\omega_c}{\omega_l}\right)^2-9a_3\left(\frac{\omega_0}{\omega_l}\right)^2+a_3\left(\frac{\omega_c}{\omega_l}\right)^2\right],$$

$$R_3=-\left[\frac{3}{4}\alpha a_2^3+\frac{3}{4}\alpha a_2^2a_4+\frac{\beta}{\gamma}a_2+\frac{3}{2}\alpha a_4^2-a_1\beta\left(\frac{\omega_c}{\omega_l}\right)^2-a_2\left(\frac{\omega_0}{\omega_l}\right)^2+a_2\beta\left(\frac{\omega_c}{\omega_l}\right)^2+a_2\beta\left(\frac{\omega_k}{\omega_l}\right)^2\right],$$

$$R_4=-\left[\frac{1}{4}\alpha a_2^3+\frac{3}{2}\alpha a_2^2a_4+\frac{\beta}{\gamma}a_4+\frac{3}{4}\alpha a_4^2-a_3\beta\left(\frac{\omega_c}{\omega_l}\right)^2-9a_4\left(\frac{\omega_0}{\omega_l}\right)^2+a_4\beta\left(\frac{\omega_c}{\omega_l}\right)^2+a_4\beta\left(\frac{\omega_k}{\omega_l}\right)^2\right],$$

$$Q_1=a_1\left(\frac{\omega_0}{\omega_l}\right)\left(\frac{\Delta\omega}{\omega_l}\right),\quad Q_2=9a_3\left(\frac{\omega_0}{\omega_l}\right)\left(\frac{\Delta\omega}{\omega_l}\right),\quad Q_3=a_2\left(\frac{\omega_0}{\omega_l}\right)\left(\frac{\Delta\omega}{\omega_l}\right),\quad Q_4=9a_4\left(\frac{\omega_0}{\omega_l}\right)\left(\frac{\Delta\omega}{\omega_l}\right). \tag{25}$$

Using the same solving processor as front, the nonlinear amplitude frequency curves of the DWNT can be determined.

4. Numerical results and discussion

4.1. The nonlinear amplitude frequency response of SWNT

Assume the linear free vibration frequency to be ω_b in Eq. (11), and $\omega_b^2=\omega_l^2+\omega_k^2$. In the numerical computation, the parameters of material and geometry are taken as $E=1.1\text{TPa}$, $\rho=1.3\times10^3\,\text{kg/m}^3$ [12], $l=45\,\text{nm}$, the outside diameter is $d_1=3\,\text{nm}$, the inside diameter is $d_0=2.32\,\text{nm}$.

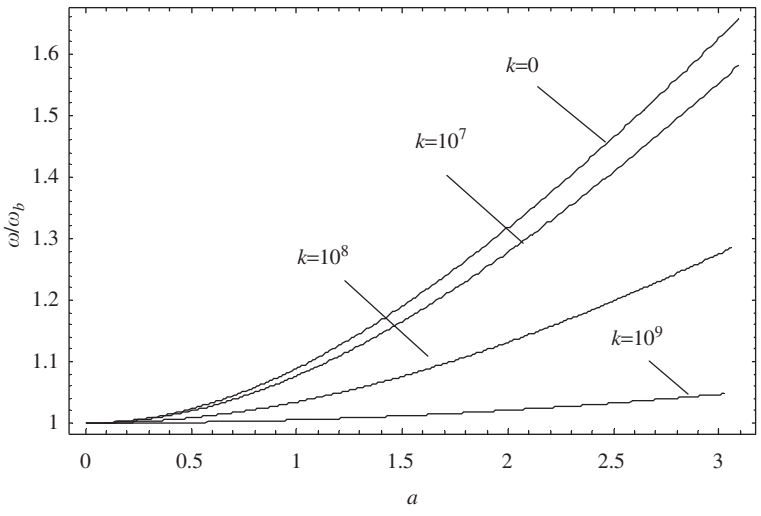

Fig. 2. Effect of spring constant k on nonlinear amplitude frequency response curves of SWNT.

Table 1
The linear free vibration frequencies ω_b of SWNT in Fig. 2

k (N/m^2)	0	10^7	10^8	10^9
ω_b (THz)	0.128	0.138	0.209	0.536

The amplitude frequency response curves of the SWNT are shown in Fig. 2 for different spring constant k. In Fig. 2, ω/ω_b is the ratio of nonlinear frequency to linear frequency, a ($a = W_{\max}/r$, $r = \sqrt{I/A} = 0.94$ nm) is the maximum dimensionless vibration amplitude. From Fig. 2, it is noted that the spring constant k of surrounding elastic medium has a pronounced effect on the nonlinear amplitude frequency response curves of SWNT. The nonlinear free vibration frequency of nanotubes rises rapidly with the increment of the vibration amplitude when the stiffness of medium is relatively small (say $k < 10^7$ N/m^2 [11,17]), in which case the variation of spring constant k has little effect on the response curves of SWNT. Consequently the effect of surrounding elastic medium can be neglected when the medium is flexible (such as a polymer medium). But following the increasing of k, the curves tend toward a flat line which indicates that the nonlinear vibration will change to linear vibration when the stiffness is large enough (say $k > 10^9$ N/m^2 [11,17]). In this case, the geometric nonlinearity of the structure deformation can be out of account.

In order to calculate the nonlinear free vibration frequency ω for different k and a, the linear free vibration frequencies ω_b are listed in Table 1.

4.2. The nonlinear amplitude frequency response of DWNT

The linear free vibration frequencies for DWNT are calculated [11] as follows:

$$\omega_{n1}^2 = \tfrac{1}{2}\left(\alpha_n - \sqrt{\alpha_n^2 - 4\beta_n}\right), \quad \omega_{n2}^2 = \tfrac{1}{2}\left(\alpha_n + \sqrt{\alpha_n^2 - 4\beta_n}\right), \tag{26}$$

where

$$\alpha_n = \frac{EI_1\lambda_n^4 + c}{\rho A_1} + \frac{EI_2\lambda_n^4 + c + k}{\rho A_2} > \sqrt{4\beta_n},$$
$$\beta_n = \frac{EI_1 EI_2\lambda_n^8}{\rho^2 A_1 A_2} + c\lambda_n^4\frac{EI_1 + EI_2}{\rho^2 A_1 A_2} + k\frac{EI_1\lambda_n^4 + c}{\rho^2 A_1 A_2}. \tag{27}$$

In the case of the DWNT with simply supported condition at the two ends, λ_n can be expressed as

$$\lambda_n l = n\pi. \tag{28}$$

Take the lowest frequency in Eq. (26) as the foundational frequency, that is $\omega_b = \omega_{11}$.

The nonlinear amplitude frequency response curves of DWNT are shown respectively in Figs. 3–5 for different spring constant k, the coefficient of the van der Waals force c and the aspect ratio l/d_2, where d_2 is the outside diameter of the outertube. In all figures, ω/ω_b is the ratio of nonlinear frequency to linear frequency, a ($a = W_{\max}/r$, $r = \sqrt{I_1/A_1} = 0.71$ nm) is the maximum dimensionless vibration amplitude, and the parameters of material and geometry are $E = 1.1$ TPa, $\rho = 1.3 \times 10^3$ kg/m^3 [13].

In Fig. 3, $c = 0.3 \times 10^{12}$ N/m^2 and the parameters of geometry are $d_2 = 3$ nm, $l = 45$ nm. It can be seen from Fig. 3 that the effect of spring constant on nonlinear vibration of DWNT is similar to that on those of SWNT (Fig. 2). In Fig. 4, the parameters are $k = 10^{17}$ N/m^2, $d_2 = 3$ nm, $l = 45$ nm. It can be seen that the nonlinear amplitude frequency response curves of the DWNTs are steep when the van der Waals forces are small, but with the increment of the forces, the curves tend towards a flat curve. In Fig. 5, the parameters are $k = 10^7$ N/m^2, $c = 0.3 \times 10^{12}$ N/m^2, $d_2 = 3$ nm. It is observed that with the increment of the aspect ratio of the nanotubes, the nonlinear vibrations frequencies of DWNTs decrease.

The linear free vibration frequencies ω_b for all cases are listed in Table 2, so it is convenient to calculate the nonlinear free vibration frequency ω for different k, c and l/d_2 in Figs. 3–5.

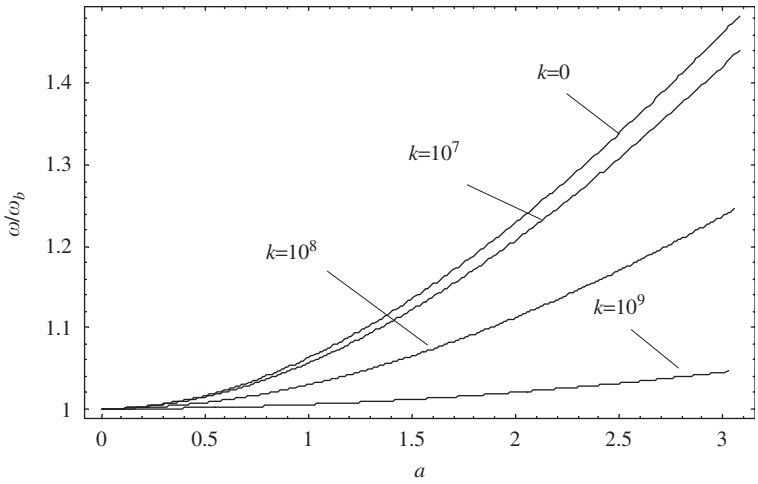

Fig. 3. Effect of spring constant k on nonlinear amplitude frequency response curves for DWNT.

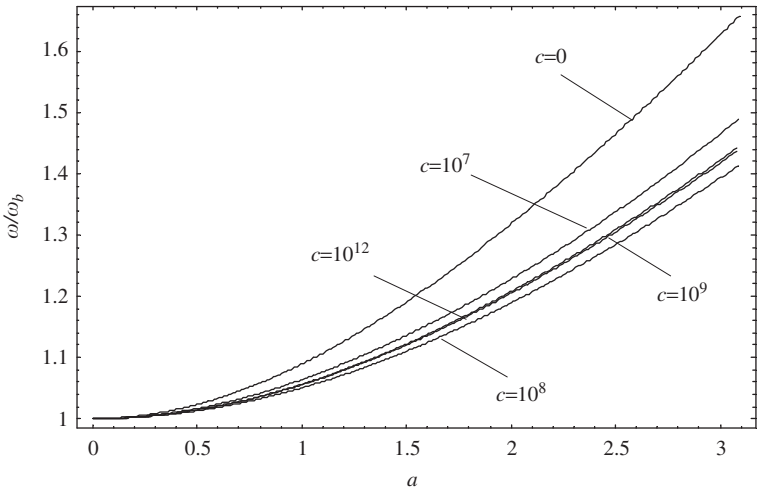

Fig. 4. Effect of coefficient of van der Waals forces c on nonlinear amplitude frequency response curves for DWNT.

5. Conclusions

In this paper, based on the continuum mechanics and a multiple-elastic beam model, a nonlinear free vibration analysis of embedded multiwall carbon nanotube considering intertube radial displacement and the related internal degrees of freedom is investigated. And the effects of the surrounding elastic medium, van der Waals forces and aspect ratio of the multiwall nanotubes on amplitude frequency response characteristics are discussed.

The present numerical results reveal that the nonlinear free vibration of nanotubes is effected significantly by surrounding elastic medium. The nonlinear free vibration frequency of nanotubes rises rapidly with the increment of the amplitude when the stiffness of medium is relatively small, but the nonlinear vibration will change to the linear vibration when the stiffness is large enough. The amplitude frequency response curves of the double-wall nanotubes are steep when the van der Waals forces are small, but with the increment of the forces, the curves tend towards a flat curve. The nonlinear vibration frequencies of double-wall nanotubes decreases with the increment of the aspect ratio of the nanotubes.

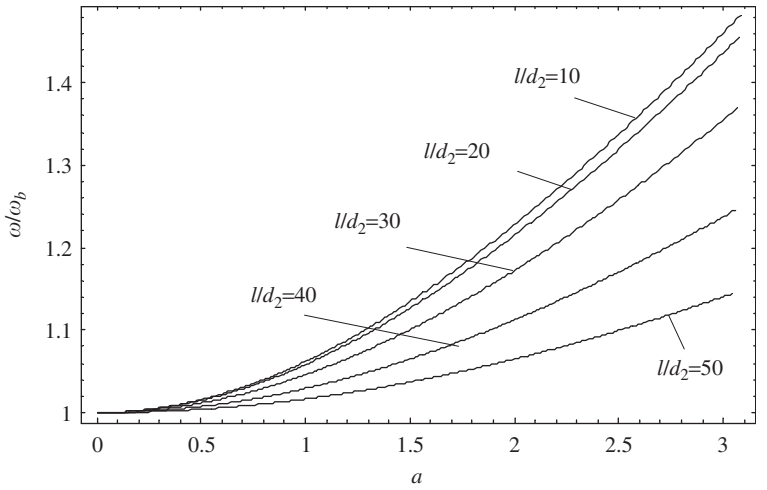

Fig. 5. Effect of aspect ratio l/d_2 on nonlinear amplitude frequency response curves for DWNT.

Table 2
The linear free vibration frequencies ω_b of DWNT in Figs. 3–5

Fig. 3		Fig. 4		Fig. 5	
k (N/m^2)	ω_b (THz)	c (N/m^2)	ω_b (THz)	l/d_2	ω_b (THz)
0	0.116	0	0.096	10	0.586
10^7	0.122	10^7	0.109	20	0.151
10^8	0.170	10^8	0.120	30	0.076
10^9	0.410	10^9	0.122	40	0.054
		10^{10}	0.122	50	0.046

References

[1] S. Iijima, Helica microtubes of graphitic carbon, *Nature* 354 (1991) 56.
[2] W. Yang, X.L. Ma, H.T. Wang, W. Hong, The advancement of nanomechanics (continued), *The Advancement of Mechanics* 33 (2) (2003) 175–185.
[3] S. Iilima, C. Brabec, A. Maiti, J. Bernholc, Structural flexibility of carbon nanotube, *Chemal Physics* 104 (1996) 2089.
[4] E.W. Wong, P.W. Sheehan, C.M. Lieber, Nanobeam mechanics: elasticity, strength, and toughness of nanorods and nanotubes, *Science* 277 (1997) 1971.
[5] J.P. Salvetal, G.A.D. Briggs, J.M. Bonard, R.R. Bacsa, A.J. Kulik, T. Stockli, N.A. Burnham, L. Forro, Elastic and shear moduli of single-walled carbon nanotube ropes, *Physical Review Letters* 82 (1999) 944.
[6] B.I. Yakobson, C.J. Brabec, J. Bernholc, Nanomechanics of carbon tubes: instabilities beyond linear response, *Physics Letters* 76 (2000) 14.
[7] O. Lourie, D.M. Cox, H.D. Wagner, Buckling and collapse of embedded carbon nanotubes, *Physical Review Letters* 81 (1998) 1638.
[8] D. Srivastava, M. Menon, K. Cho, Nanoplasticity of single-wall carbon nanotubes under uniaxial compression, *Physical Review Letters* 83 (1999) 2973.
[9] T. Ozaki, Y. Iwasa, T. Mitani, Stiffness of single-walled carbon nanotubes under large strain, *Physical Review Letters* 84 (2000) 1712.
[10] C.Q. Ru, Column buckling of multiwall carbon nanotubes with interlayer radial displacements, *Physical Review B* 62 (2000) 16962–16967.
[11] J. Yoon, C.Q. Ru, A. Mioduchowski, Vibration of an embedded multiwall carbon nanotube[J], *Composites Science and Technology* 63 (2003) 1533–1542.
[12] A. Pantano, M.C. Boyce, D.M. Parks, Nonlinear structural mechanics based modeling of carbon nanotube deformation, *Physical Review Letters* 91 (14) (2003) 145501-1–145501-4.
[13] C.Q. Ru, Elastic buckling of single-walled carbon nanotube ropes under high pressure, *Physical Review B* 62 (2000) 15.

[14] Y. Lanir, Y.C.B. Fung, Fiber composite columns under compressions, *Journal of Composite Materials* 6 (1972) 387–401.
[15] H.T. Hahn, J.G. Williams, Compression failure mechanisms in unidirectional composites, *Composite Materials: Testing and Design* 7 (1984) 115–139.
[16] S.L. Lan, Y.K. Cheung, Amplitude Incremental variational principle for nonlinear vibration of elastic systems, *Journal of Applied Mechanics* 48 (1981) 959–964.
[17] Y. Lanir, Y.C.B. Fung, Fiber composite columns under compressions, *Journal of Composite Materials* 6 (1972) 387–401.